Flow, Turbulence and Combustion **63:** 269–291, 1999.

Approximate Wall Boundary Conditions in the Large-Eddy Simulation of High Reynolds Number Flow

W. CABOT and P. MOIN
Center for Turbulence Research, Stanford University, Bldg. 500, 488 Escondido Mall, Stanford, CA 94305-3030, U.S.A.

Abstract. The near-wall regions of high Reynolds numbers turbulent flows must be modelled to treat many practical engineering and aeronautical applications. In this review we examine results from simulations of both attached and separated flows on coarse grids in which the near-wall regions are not resolved and are instead represented by approximate wall boundary conditions. The simulations use the dynamic Smagorinsky subgrid-scale model and a second-order finite-difference method. Typical results are found to be mixed, with acceptable results found in many cases in the core of the flow far from the walls, provided there is adequate numerical resolution, but with poorer results generally found near the wall. Deficiencies in this approach are caused in part by both inaccuracies in subgrid-scale modelling and numerical errors in the low-order finite-difference method on coarse near-wall grids, which should be taken into account when constructing models and performing large-eddy simulation on coarse grids. A promising new method for developing wall models from optimal control theory is also discussed.

Key words: turbulence, large-eddy simulation, wall models, channel flow, separation.

Abbreviations: DNS – direct numerical simulation; LES – large-eddy simulation; RANS – Reynolds-averaged Navier–Stokes; SGS – subgrid-scale; TBLE – thin boundary layer equations

Nomenclature

A^+	=	damping function parameter
B	=	log law intercept
C	=	dynamic coefficient for the Smagorinsky model
C_f	=	friction coefficient, $2\tau_w/U_\infty^2$
C_p	=	relative wall pressure coefficient, $2(P_w - P_o)/U_\infty^2$
h	=	step height
k	=	turbulent kinetic energy
L	=	inertial length scale, k/ε
$\mathcal{L}$	=	residual SGS stress between test and grid filter levels
$\mathcal{M}$	=	residual SGS model strain between test and grid filter levels
P	=	mean pressure
P_m	=	matching pressure at y_m
Re_h	=	step Reynolds number, $U_\infty h/\nu$

Re_τ = friction Reynolds number, $u_\tau \delta/\nu$
$\mathbf{S}$ = strain rate tensor
$\mathcal{T}$ = residual SGS stress at test filter level
U = mean streamwise velocity
u' = streamwise rms velocity fluctuation intensity
$\widetilde{u}_j$ = velocity in the inner layer
U_∞ = free stream velocity
U_m = streamwise matching velocity at y_m
U_{mi} = matching velocity at y_m in the ith direction
u_τ = friction speed
x = streamwise coordinate
y = wall-normal coordinate
y^+ = wall-normal coordinate in wall units, yu_τ/ν
y_m = matching height
δ = channel half-width or boundary layer thickness
Δ = effective filter width
ε = turbulent dissipation rate
κ = von Kármán constant, inverse slope of log law
ν = kinematic coefficient of molecular viscosity
ν_s = SGS eddy viscosity
ν_t = eddy viscosity in the inner layer
τ = residual SGS stress at grid filter level
τ_w = streamwise wall stress
τ_{wi} = wall stress in the ith direction

1. Introduction

The near-wall region in high Reynolds number turbulent flow contains small vortical structures (streaks) that are dynamically important to the flow, but which have dimensions that scale with the viscous scale, making it impractical to resolve them in numerical simulations at very high Reynolds numbers. Thus there is a crucial need to approximate the overall dynamical effects of the streaks on the larger outer scales through appropriate boundary conditions without resolving the inner viscous regions. On the other hand, the need for approximate wall boundary conditions has not been so well established in separated flow regions, which do not exhibit this streak-like structure, and which behave effectively like low Reynolds numbers flows with lower resolution requirements.

In 1970, Deardorff [17], constrained by the limited computing power of his time, performed a large-eddy simulation (LES) of channel flow with no molecular viscosity on a very coarse grid. He used approximate boundary conditions, matching the second wall-normal derivatives to the log law values, and an eddy viscosity subgrid-scale (SGS) model, with which he obtained fairly poor mean flow statistics. The same near-wall resolution problem presents itself to us today, even though we have vastly greater computing power than in 1970, as we attempt to simulate more complex, high Reynolds number flows.

1.1. LES RESOLUTION ISSUES

Current subgrid-scale models, which generally do a good job predicting unresolved turbulent dissipation, do not model unresolved stresses accurately when they are a significant fraction of the total Reynolds stress [28]. As a consequence, a proper LES must resolve all "large" turbulent scales in the flow, viz., those that contain most of the turbulent kinetic energy and Reynolds shear stress in a localized region of the flow. Another way to put this is that the grid spacing Δ should be some minimal ratio of the local inertial length scale, $L = k^{3/2}/\varepsilon$, where k is the turbulent kinetic energy and ε is the turbulent dissipation rate; this ratio has been estimated to be $\Delta/L \approx 1/10$ to obtain good results in channel flow [4]. Near walls in boundary layers the size of turbulent eddies scales roughly as the distance from the wall, limited by viscous scales, which means that well resolved LES requires grids nearly as fine as those used in direct numerical simulation (DNS). This restriction applies not only to wall-normal grid spacing but to horizontal grid spacing as well. Baggett et al. [4] estimated that the number of grid points necessary to resolve a channel flow properly with LES scales approximately as Re_τ^2. In well resolved LES of wall-bounded flow, most of the grid points are thus used in the near-wall regions. An example of this is a simulation with zonal refinement near the walls at a modest friction Reynolds number $\mathrm{Re}_\tau = 1000$ [27], in which 70% of grid points were allocated in near-wall zones comprising only 10% of the channel width. The time step in the simulations must also be decreased accordingly with these finer grids for numerical stability.

We note that, in practice, many LES applications use fairly coarse horizontal grids – too coarse in fact to resolve the energy-containing scales accurately – but refine the grid in the wall-normal direction to nearly DNS accuracy to "resolve" the buffer and viscous regions; we will refer to such simulations as "wall-resolved" simulations as opposed to ones, e.g., using refined zonal meshes, that are *well resolved* in all directions.

Near-wall resolution requirements clearly limit the application of LES to moderate Reynolds number flows, even on current supercomputers, and a modelling strategy for the near-wall region needs to be devised if LES is to be applied to many practical applications. The ultimate goal of wall modelling is to develop approximate boundary conditions near walls that allow one to use LES grids that scale only on outer flow scales, such as the boundary layer thickness in attached flow, and whose wall modelling expense is at most only weakly dependent on Reynolds numbers.

1.2. WALL STRESS MODELS

Approximate wall boundary conditions that supply wall stresses to the LES from the unresolved wall were used in 1975 by Schumann [42] and are still used in various modified forms. We refer to this general class of boundary condition as "wall stress models". The wall stress or drag cannot be computed accurately on

very coarse wall-normal grids that extend to the wall and must be determined from models matched to outer flow conditions. Schumann, using a finite volume code, applied wall stresses, based on the known steady-state result to the wall faces of his control volumes. Grötzbach [22] later modified this to use the instantaneous fit of the log law to the mean velocity profile. Such wall models based on the law of the wall have been used extensively over the years for both attached and separated flow calculations, even though not valid for the latter. Piomelli et al. [40] modified Schumann's approach by shifting the interior horizontal velocity and wall stress by an empirical amount to approximate the tilting of eddies near the wall, as well as a model that included a term with the wall-normal velocity to approximate the effects of bursts and sweeps at the wall. Both models were found to improve the channel flow results slightly. Nonstandard log law coefficients can be fit to outer flow profiles in flows with significant pressure gradients and used to predict wall stresses. Recently, temporally evolving thin boundary layer equations (TBLE), with coarse near-wall resolution parallel to the wall, have been used [8, 9, 11, 12] to predict wall stresses in LES of attached and separated flows, with improved results in some cases. TBLE are essentially the Navier-Stokes equations neglecting the horizontal viscous diffusion terms and fixing the pressure gradient to the outer flow value.

In very coarse LES of attached flow with wall stress models, one generally finds that the core flow far form the walls can be predicted with fair accuracy in many cases, but that the flow very near the wall is poorly predicted, which can in turn adversely influence physical processes like boundary layer growth and separation that depend strongly on the characteristics of the momentum flux near the wall.

1.3. Off-wall boundary conditions

Another superficially attractive approach is to apply approximate wall boundary conditions directly on the velocity field at some height above the physical location of the wall. The main reason for this is that in most of the previously cited examples the LES grid is too coarse in the near-wall region in both the wall-normal and horizontal directions to capture the energy-bearing scales of motion or even the variation of the mean flow in the wall-normal direction. With a zonal or unstructured mesh, one could provide a mesh for the outer flow that does capture the energy-containing scales down to a certain distance from the wall that is physically reasonable (say, within some small fraction of the boundary layer thickness) and affordable for the given computational resources. Boundary conditions on all velocity components are then specified at the location off of the wall where the grid ends.

Attempts at using such "off-wall" boundary conditions synthesized from rescaled interior flow data [7, 29, 36] have proven to be largely unsuccessful. Baggett [5] performed tests using exact near-wall flow data in a channel, obtained from a wall-resolved LES, as an off-wall boundary condition; by scrambling the phases

of the data, he found that the interior flow was severely disrupted near the artificial boundary unless the relative phases and the time scales of the original flow were preserved in the boundary plane, indicating that a good deal of physical structural information is required for off-wall boundary conditions to avoid generating spurious transition regions. Jiménez and Vasco [29] found that the interior flow is very sensitive to the boundary-normal transpiration velocity; if it is incompatible in the sense of continuity from the interior flow, then large pressure and velocity fluctuations are generated. The off-wall boundary may also be generally incompatible in the sense of injecting an unphysical rate of energy into the interior flow; this may also be a problem in wall stress models. Any workable off-wall model will need to satisfy rather severe constraints like this, which makes them very difficult to construct successfully.

The usual result of applying poorly designed off-wall boundary conditions is the appearance of a strong, spurious boundary layer above the artificial boundary. The rest of the outer flow may also be affected adversely in addition because of the spurious pressure generated at the artificial boundary, which is felt everywhere in incompressible flow. Because of these problems, we will restrict our further discussion to the performance of wall stress models.

1.4. Numerical scheme

Throughout this paper we will discuss results using second-order central finite differencing on a staggered grid [23, 25] and a third-order Runge-Kutta time advancement scheme, whose numerical properties have been examined in some detail [15, 20, 26, 32]. Numerical dispersion errors are known to be high for second-order differencing, which effectively reduces the spatial resolution to about 1/3 that of spectral methods for same number of grid points in each direction [32], and in which numerical errors are probably comparable to the contributions from the SGS model [20]. However, low-order codes like these have good conservation properties, are relatively flexible for implementation in complex geometries, and are hence widely used in engineering flow applications. It is therefore of practical interest to examine their performance using LES on coarse grids with wall models. We will also only consider simulations using the standard dynamic SGS model [19, 31]. These choices, as will be seen further on, have important consequences on the wall model results.

1.5. Outline

In this paper, we review recent simulation results from coarse LES using wall stress models to examine their performance and identify sources of error that may lead to the generally poor results found close to the wall. In particular, the lack of resolution of energy-containing scales of motion, the behaviour of SGS models on coarse grids near walls and the numerical solution technique contribute to these

errors. New wall modelling strategies that make use of tools from control theory [37, 38] will also be discussed that attempt to correct, or at least work around, these deficiencies. In Section 2 results from LES using specific types of wall stress models in attached and separated turbulent flow are presented and discussed, and new strategies for developing wall models are discussed. In Section 4 we conclude with a discussion of practical ways to implement wall models in their current state.

2. Wall Stress Models

The objective with wall stress models is to supply to the simulation of the outer flow the viscous stresses or drag due to the sharp velocity gradient at the walls, which cannot otherwise be calculated on the very coarse LES grid. Wall stress models generally use information from outer flow near the wall to set the level of wall stress, which allows them to respond to varying conditions in the outer flow. Depending on the level of modelling effort, the wall stress can be determined from an algebraic model, or from differential model equations on a grid refined in the wall-normal direction. The wall stress is in turn fed back to the outer flow LES as an additional drag in the near-wall cells. In second-order finite difference or finite volume approaches the horizontal velocities on the wall, normally needed to compute the viscous stresses, are not used and can be considered to be slip velocities. The wall-normal velocity in the outer flow is taken to be zero at the wall. There is an implicit assumption made that the Reynolds stresses near the wall in the outer flow can be accurately calculated from the SGS model and resolved flow field, although this is usually far from true on coarse grids.

2.1. Wall stresses based on the law of the wall

For attached flow at sufficiently high Reynolds number, the first off-wall computational cells extend into the logarithmic region, and the horizontal velocity (either the instantaneous values or some kind of spatial or temporal mean) can be fitted to the log law to predict a wall stress. Tests of wind tunnel data [35] show, however, that an instantaneous logarithmic region is valid only on horizontal scales greater than about 1800 wall units. This can take the simple form

$$U_m = u_\tau \left[\kappa^{-1} \ln(y_m u_\tau/\nu) + B\right], \quad \tau_w = u_\tau^2, \tag{1}$$

where U_m is the instantaneous horizontal speed in the outer flow at a distance y_m from the wall, τ_w is the wall stress, u_τ is the friction speed, ν is the kinematic coefficient of molecular viscosity, $\kappa \approx 0.4$ is von Kármán's constant, and $B \approx 5$ is the log law intercept; or a more complicated composite formula for u_τ including the viscous and "wake" regions [16] can solved in flows featuring low Reynolds number regions (e.g., near separation). For rough walls, the value of the matching height y_m is usually offset by an effective roughness thickness [33]. These equations are generally transcendental in u_τ, but can be solved quite efficiently

with a few Newton iterations. Sometimes Equation (1) is applied only to the mean streamwise component of velocity in simple flows [22, 42], or an effort is made to calculate the wall stress in alignment with the full horizontal velocity [11, 33]. Because flow conditions at a height y_m affect the wall some distance downstream, one can shift U_m and τ_w either manually by an empirical amount [40] or by time averaging the matching velocity from the outer flow over roughly the diffusion time of the inner layer. This shift is seen to increase the correlation of U_m and τ_w in *a priori* tests of resolved flow simulations from about 30 to 50%, and slight improvements in the mean flow results have been reported [40]. Note that the level of averaging used in specifying U_m affects the calibration of log law constants in Equation (1) [33]. Werner and Wengle [47] fit the instantaneous horizontal velocities to a profile comprising a power law (rather than a log law) matched to a linear near-wall segment to obtain wall stresses, which does not give significantly different wall stress predictions from the previously cited models; for the subgrid-scale eddy viscosity they also switched from a Smagorinsky model to a mixing length model near walls.

In geometrically simple flows like channel, horizontally averaged U_m can be used to set a mean τ_w, with fluctuations set equal to the near-wall velocity fluctuations [22, 42]. Wu and Squires [48] generalized this approach to complex boundaries by obtaining a steady RANS solution for the near-wall region to determine the mean wall stress and using instantaneous outer flow information to set the local fluctuations in the wall stress.

2.2. WALL STRESSES USING THIN BOUNDARY LAYER EQUATIONS

The unsteady thin boundary layer equations (TBLE), which in general are a simplified set of partial differential equations derived from the Navier–Stokes equations, can also be used, especially in flows with large pressure gradients which require more detailed momentum balance information [8]. The governing equations for inner horizontal velocity components $\widetilde{u}_i$ $(i = 1, 3)$ are

$$\frac{\partial \widetilde{u}_i}{\partial t} + \frac{\partial (\widetilde{u}_i \widetilde{u}_j)}{\partial x_j} + \frac{\partial P_m}{\partial x_i} = \frac{\partial}{\partial y}\left[(\nu + \nu_t)\frac{\partial \widetilde{u}_i}{\partial y}\right] \tag{2}$$

with continuity

$$\widetilde{u}_2 = -\int_0^y \frac{\partial \widetilde{u}_i}{\partial x_i}\,\mathrm{d}y', \tag{3}$$

and with matching interior boundary condition $\widetilde{u}_i(y_m) = U_{mi}$ and wall boundary condition $\widetilde{u}_i(0) = 0$. In Equation (2), P_m is the near-wall pressure from the outer flow, assumed to be independent of y in the inner layer. The eddy viscosity ν_t is usually modelled with an ad hoc damped mixing length prescription that approxim-

ates the linear and logarithmic regions for attached flow with reasonable accuracy. Balaras et al. [8, 9] used

$$\nu_t = (\kappa y)^2 |\widetilde{\mathbf{S}}| D, \quad D = [1 - \exp(-(y^+/A^+)^3)], \tag{4}$$

where $|\widetilde{\mathbf{S}}|$ is the magnitude of the strain rate, y^+ is the distance from the wall in wall units, and $A^+ = 25$. Cabot [11, 12] used

$$\nu_t = \kappa y u_\tau D, \quad D = [1 - \exp(-y^+/A^+)]^2, \tag{5}$$

with $A^+ = 17$. The wall-normal velocity given by Equation (3) does not in general match that of the outer flow at the matching point y_m; these can be made consistent, however, by imposing the condition that the horizontal mass flux in the inner layer also agrees with that in the outer flow, instead of matching the horizontal velocity itself. Finally, the wall stress is determined from the wall gradient of the inner solution:

$$\tau_{wi} = \nu \left. \frac{\partial \widetilde{u}_i}{\partial y} \right|_{y=0}. \tag{6}$$

The solution of Equation (2) is generally found on a grid embedded within the outer LES grid that is refined in the wall-normal direction such that the viscous region is resolved well enough to compute the wall stress directly from Equation (6). The horizontal resolution in the inner region is taken to be the same or even coarser than the outer solution, justifying to some extent using inner governing equations that resemble Reynolds-averaged Navier–Stokes (RANS) models. However, we have found no significant difference between results using horizontal grids that are the same as the outer grid and ones twice as coarse [11, 12].

When the left-hand side of Equation (2) is set to zero, we refer to it as the "stress balance model", which are solutions of uncoupled ordinary differential equations in each near-wall computational cell that vary smoothly between a linear and logarithmic solution, and which can be solved numerically at little expense with a semi-analytic solution. In attached flow at high Reynolds numbers, the stress balance model is equivalent to the instantaneous log law model (Equation (1)). The left-hand side (or selected terms therein) can also be approximated by values from the outer flow; e.g., Hoffmann and Benocci [24] suggested using only the pressure gradient and time-derivative of the velocity. Wall stress models using the full, time-evolving solution of Equation (2) are called "thin boundary layer equation models" [12] or "two-layer models" [9]. It was noted by Cabot [12] that the Reynolds stress carried by the nonlinear terms in Equation (2) are substantial and that a lower value of eddy viscosity should be used in principle, corresponding to a lower value of κ in Equations (4, 5).

Instantaneous and shifted wall stress models based on algebraic or semi-analytic representations of the log law are attractive because they are simple and very inexpensive to compute. Unsteady boundary layer equations are about half as expensive to compute as the full Navier–Stokes equations for the same number of grid points,

and the fine wall-normal resolution required makes them very much Reynolds number dependent – not a good feature when going to very high Reynolds number applications. They are, however, in principle more accurate and flexible in complex flow situations. And, while the mixing length eddy viscosity model normally used in all of these models is not valid in separated and reattaching regions, it has certainly not prevented their use in these cases, with surprisingly good success under the circumstances (see Section 3.2). The cost of computing the LES of the outer flow, of course, decreases dramatically using wall stress models, since much coarser grids can be used near walls and, for explicit numerical schemes, larger time steps can be used. The precise savings one gains in computational cost depends very much on the complexity of the flow and the complexity of the wall model employed.

2.3. SUBGRID-SCALE MODELLING

In the simulations we will be considering, the standard dynamic procedure is applied to the Smagorinsky [43] SGS model for the trace-free (*) part of the residual stress τ [19, 31]:

$$\tau^* = (\overline{\mathbf{u}\mathbf{u}} - \overline{\mathbf{u}}\,\overline{\mathbf{u}})^* \sim -2\nu_s\overline{\mathbf{S}} = -2C\Delta^2|\overline{\mathbf{S}}|\overline{\mathbf{S}}, \tag{7}$$

where $\overline{(\ )}$ denotes the filter, ν_s is the SGS eddy viscosity, C is the Smagorinsky coefficient, Δ is the effective grid width, and $\overline{\mathbf{S}}$ is the resolved strain tensor. At a coarser scale given by an additional test filter $\widehat{(\ )}$, the residual stress is

$$\mathcal{T}^* = (\widehat{\overline{\mathbf{u}\mathbf{u}}} - \widehat{\overline{\mathbf{u}}}\,\widehat{\overline{\mathbf{u}}})^* \sim -2\widehat{\nu}_s\widehat{\overline{\mathbf{S}}} = -2C\widehat{\Delta}^2|\widehat{\overline{\mathbf{S}}}|\widehat{\overline{\mathbf{S}}}. \tag{8}$$

Test filtering Equation (7) and combining with (8), assuming that C is not affected by the filtering operation, gives an algebraic expression for C in terms of test-filtered flow quantities, which is solved in a least-squares sense over tensor components and a spatial average $\langle\ \rangle$:

$$C \sim \langle \mathcal{L} : \mathcal{M}\rangle / \langle \mathcal{M} : \mathcal{M}\rangle, \tag{9}$$

where

$$\mathcal{L} \equiv (\widehat{\overline{\mathbf{u}}\,\overline{\mathbf{u}}} - \widehat{\overline{\mathbf{u}}}\,\widehat{\overline{\mathbf{u}}})^*, \quad \mathcal{M} \equiv 2(\Delta^2|\widehat{\overline{\mathbf{S}}}|\widehat{\overline{\mathbf{S}}} - \widehat{\Delta}^2|\widehat{\overline{\mathbf{S}}}|\widehat{\overline{\mathbf{S}}}). \tag{10}$$

A more mathematically rigorous formulation of the dynamic procedure, including effects of backscatter, is provided by Ghosal and Moin [21].

In plane-parallel flows, filtering and averaging are performed only on horizontal planes parallel to the walls. When the simulation uses a refined wall-normal grid, this may be justified, since the filtering over very small wall-normal distances has little effect. This approach is not at all justified when the mesh is so coarse in the wall-normal directions that large flow variations are being averaged over. The general class of commutative filters developed by Vasilyev et al. [45], which is

normally applicable to all directions in wall bounded flows, is not appropriate here for the same reason. Also the terms used to compute C in the dynamic procedure, especially strain terms involving wall-normal derivatives, cannot be determined accurately on a coarse grid near walls. We therefore recognize from the outset that the SGS model may be highly inaccurate in the near-wall region, and that improvements are clearly needed in SGS/wall modelling in this area.

When filters are much wider than energy-containing scales, as is the case on coarse near-wall meshes, one expects that the effect of large-scale spatial averaging over many turbulent eddies might correspond to a Reynolds average. In that case, one would be justified in switching from SGS models suited for isotropic flow conditions to a RANS-like solution in the near-wall region. Baggett [6] has shown that it is difficult to merge the RANS and SGS eddy viscosities without generating an artificial buffer region between an effectively low Reynolds number flow near the wall and the outer flow.

There are several other issues that affect the accuracy of the SGS model on coarse grids. The Smagorinsky model, while adequate for predicting SGS dissipation in fairly isotropic turbulent regions, does not carry sufficient stresses, and it cannot treat cases with large degrees of anisotropy [28], both of which are important factors near walls. The numerical errors in second-order finite differencing are probably comparable to the contribution from the SGS model [20]. This further affects the dynamic procedure, because it samples the highest resolved wavenumbers, which are probably contaminated by dispersion errors [32]. It has also been noticed recently that the value of the Smagorinsky coefficient and eddy viscosity drop dramatically near the wall in the outer flow, which has been found to be occur on the first few grid cells away from the wall regardless of the physical grid spacing [41]. This unphysical behaviour may result from applying the dynamic procedure inappropriately to energy-bearing scales where the self-similarity assumptions break down. We will show in Section 3.1 that the level of the near-wall SGS eddy viscosity can have a large effect on the results. A rather complicated attempt to improve the near-wall SGS model prediction [44] uses a nested grid along the wall and directly computes the residual Reynolds stresses, with model inaccuracies occurring at the nested grid level.

3. Results

3.1. CHANNEL FLOW

Results are shown here for very coarse LES with 32^3 computational cells with the second-order central finite difference code for $\mathrm{Re}_\tau = 4000$ and 20000 [14]. The numerical domain is $2\pi \times 2 \times 2\pi/3$ in the streamwise, wall-normal and spanwise directions in units of channel half-width δ. This domain size is considered to be marginally adequate to capture the largest structures in the core of the flow, a typical symptom of which is an exaggerated wake region [27]. While this resolution may seem exceptionally coarse, it is probably representative of resolutions

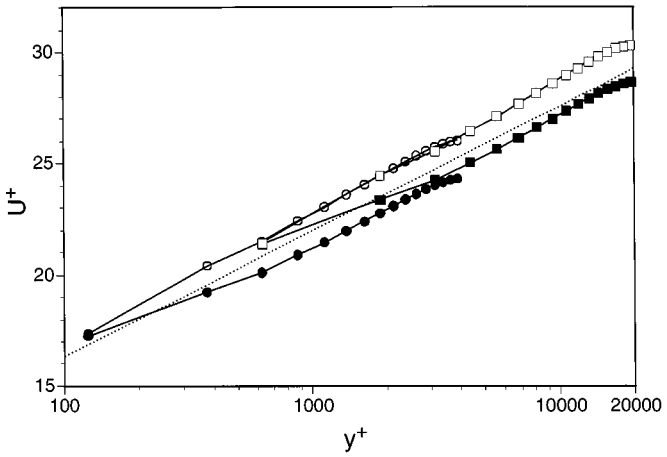

Figure 1. Mean streamwise velocity in wall units for LES with TBLE wall stress models on a 32^3 mesh at $\mathrm{Re}_\tau = 4000$ (circles) and 20000 (squares) with (open symbols) and without (solid symbols) enhanced SGS eddy viscosity near the walls. The log law (Equation (1)) using $\kappa = 0.41$ and $B = 5.1$ is also shown (dotted line).

that must be used in high Reynolds numbers, complex flow configurations. Mean velocity results are largely insensitive to the type of wall stress model. The wall stress was computed using the instantaneous log law model (Equation (1)) and the full thin boundary layer equations (Equation (2)) [11, 14], and using a shifted log law model [37, 38], with little significant difference between any of the results. The horizontal velocity from the centre of the first off-wall computational cell was used to compute the wall stresses.

In the first two or three grid points adjacent to the walls, the results are generally poor for the mean streamwise velocity U using the standard dynamic SGS model, as seen in Figure 1 (solid symbols). The slope of U in the first few off-wall grid points changes from interior values and is much too shallow. Because this is the region in which the outer flow is matched to the inner solution, it causes the logarithmic region to have too low an intercept. As a consequence, the mass flux will also tend to be too low for the predicted skin friction, or equivalently the skin friction will be too high for a given mass flux or free stream velocity. The near-wall anisotropy of the resolved flow is also not well predicted, with values of the streamwise velocity fluctuation intensity u' that are somewhat too high, again most noticeably at the first few off-wall grid points. This is shown in Figure 2 with reference to a well resolved LES [27], in which more scales are resolved compared with the coarse LES (especially near the walls) and which should therefore have larger intensities. Note that the tendency to overpredict streamwise fluctuations is also a well known problem in "wall-resolved" simulations that do not properly resolve the horizontal scales near walls [27]. It was found [37, 38] that matching the wall stress model to the horizontal velocity at a height above the spurious near-wall points effectively shifts U profile to the proper level, with the first few off-wall

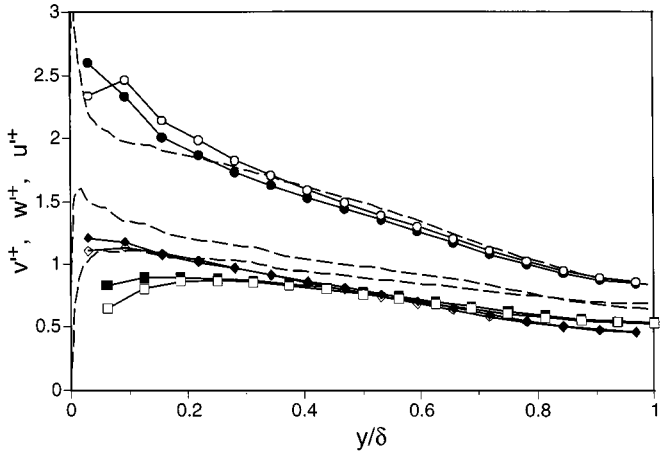

Figure 2. Resolved velocity fluctuation intensities for LES with TBLE wall stress models on a 32^3 mesh at $\mathrm{Re}_\tau = 4000$ with (open symbols) and without (solid symbols) enhanced SGS eddy viscosity near the walls. For comparison the (unfiltered) well resolved LES data of [27] at $\mathrm{Re}_\tau = 4000$ is shown with dashed lines.

points now having values that are too large. The mean streamwise momentum balance,

$$\tau_w \approx (\nu + \nu_s)\,\mathrm{d}U/\mathrm{d}y - \overline{u'v'} - (\mathrm{d}P/\mathrm{d}x)y, \tag{11}$$

where $\mathrm{d}P/\mathrm{d}x$ is the mean pressure gradient and $-\overline{u'v'}$ is the resolved Reynolds stress, is largely insensitive to the level of U. It was found that $\mathrm{d}U/\mathrm{d}y$ could be steepened in the near-wall region by augmenting SGS eddy viscosity ν_s in the near-wall region [6]. This has the effect of lowering the resolved velocity fluctuations and hence $-\overline{u'v'}$ substantially, which appear to be overpredicted, even though it raises the value of $\nu_s dU/dy$ at the same time by a smaller amount.

It was found [14] that modifying the values for the dynamic coefficient C in the SGS model (7) at the first three off-wall points with a linear fit to interior values gives much higher SGS eddy viscosities near the wall (Figure 3) and improves somewhat the near-wall behaviour of the mean streamwise profile (Figure 1). (Interior plane-averaged values of C for $y/\delta < 0.6$, excluding the three near-wall points, were used for the fit; they were found to be sufficiently smooth to give well behaved solutions without additional time averaging.) This fix is partially justified by the consideration that the near-wall computational cells still lie well in log layer and Reynolds stresses should not be affected strongly by the presence of the wall. The improvement in the mean velocity results indicate that the under-resolved flow and inaccuracies in standard SGS models in the vicinity of walls contribute to poor predictions of dissipation and Reynolds stresses there. We note that the mixed dynamic SGS model [50], which includes a self-similar stress term, $\overline{\overline{\mathbf{u}}\,\overline{\mathbf{u}}} - \overline{\mathbf{u}}\,\overline{\mathbf{u}}$, in the model for the residual stress (Equation (7)), performs worse at these coarse resolutions, because it tends to give larger residual stresses and lower

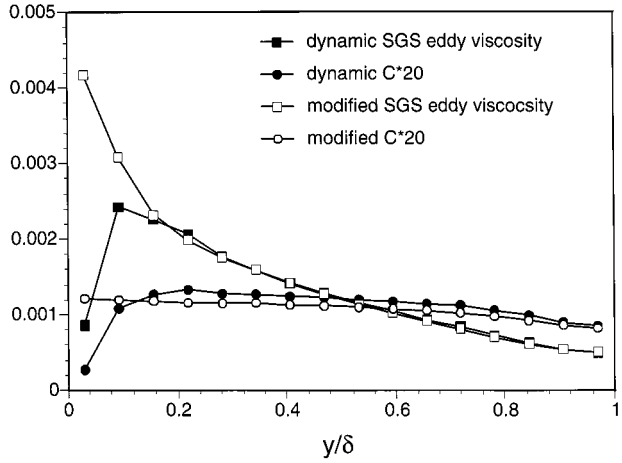

Figure 3. The mean SGS eddy viscosity ν_s in units of $u_\tau \delta$ (squares) and the coefficient $20C\Delta^2/\delta^2$ (circles) from the dynamic Smagorinsky model (Equation (7)) for LES on a 32^3 mesh at $\mathrm{Re}_\tau = 4000$ (solid symbols). The curves with open symbols are modified by fitting the three near-wall points of C linearly to interior values.

eddy viscosity (dissipation), which acts entirely in the wrong direction. There is no real overall improvement in the rms velocities by enhancing the near-wall SGS eddy viscosity (Figure 2); the shift outward in the peak of u' may indicate that the near-wall flow is just acting like a lower Reynolds number flow [6].

Another problem appears to be the development of unphysical structures near the wall. Baggett [6] showed that streak-like structures develop near the walls with maximum spanwise spacing of about six times the grid spacing or the physical scale, which is about 100 wall units. In moderately high Reynolds number LES the grid spacing is several hundred of wall units or greater, but the robust streak formation process causes streaks to develop with unphysically large dimensions, giving rise to unphysical velocity intensities and correlations. These structures occur in the previously presented simulations and may account in part for the inaccurate rms velocity fluctuations predicted near the walls. In this context it is interesting to note that Mason and Thomson [34] added stochastic fluctuations to the SGS model, which improved the mean velocity profiles near the walls. It is possible that the improvement occurs because the stochastic fluctuations disrupt the development of these pseudo-streaks, although this needs to be verified with more careful studies.

A notable feature about the mean streamwise velocity profiles using wall models is that they exhibit virtually no wake-like structure in the core compared with experimental data and results from better resolved simulations. This behaviour occurs for both 32^3 and 64^3 resolutions [14] and appears to be insensitive to the type of wall stress model and near-wall enhancement of the SGS eddy viscosity, even with quite vigorous wall stress fluctuations [37, 38]. A physical analogy to changing the wall conditions is the difference between smooth and rough walls.

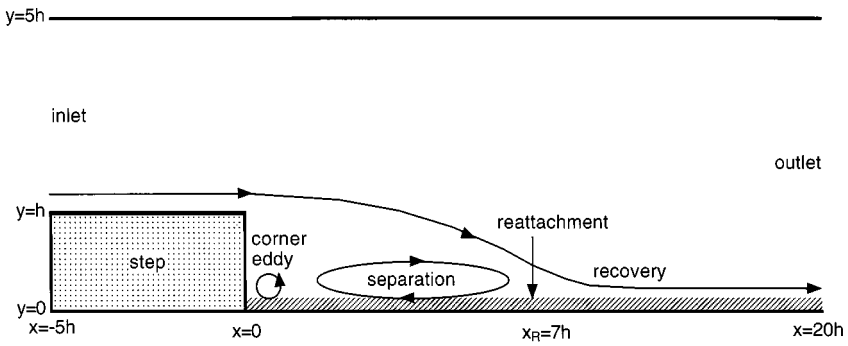

Figure 4. Sketch of the simulation domain for flow over a step of height h with an expansion ratio of 4 to 5. Wall stress models were used in the hatched region.

Perry et al.'s [1, 39] data show a slight drop in the wake parameter for rough walls, but nothing nearly as dramatic as seen in the coarse LES results. The lack of a wake appears instead to be due to insufficient resolution of the core flow with low-order numerical schemes. A healthy wake was recovered at $\mathrm{Re}_\tau = 2000$ with the same numerical scheme with resolved walls [32] only when the grid spacing was about five times finer in the streamwise and ten times finer in the spanwise directions than on the coarse 32^3 grid used here. This demonstrates the degree to which the second-order numerical scheme degrades the resolution of the simulation.

3.2. SEPARATED FLOW

Arnal and Friedrich [3] performed LES of flow over a step on a coarse grid using the dynamic SGS model and a law-of-the-wall wall stress model [42] on all of the solid boundaries. They found quantitatively good results for $\mathrm{Re}_h = 113{,}000$ and 1:2 expansion ratio compared with experimental results, but their prediction of the reattachment point was poor.

Several wall stress models were employed [12, 13] on a coarse grid on the bottom wall behind a step with otherwise the same numerical setup and inflow conditions as [2] for the case with $\mathrm{Re}_h = 28000$ and 4:5 expansion ratio (see the sketch in Figure 4). Only 8 computational cells in the wall-normal direction with uniform spacing were used from the bottom wall to half way up the step, compared with 16 computational cells on a stretched mesh used in the wall-resolved case [2]. The flow in the wall-resolved LES reattaches at about 6.5 step heights (h) past the step. A massive separation bubble develops between about 2.5 and $6.5h$, with progressively smaller secondary and tertiary recirculation bubbles in the corner underneath the step within $0.5h$ of the step location. The standard dynamic Smagorinsky SGS model was used with filtering on planes parallel to the bottom wall and with averaging in the homogeneous spanwise direction.

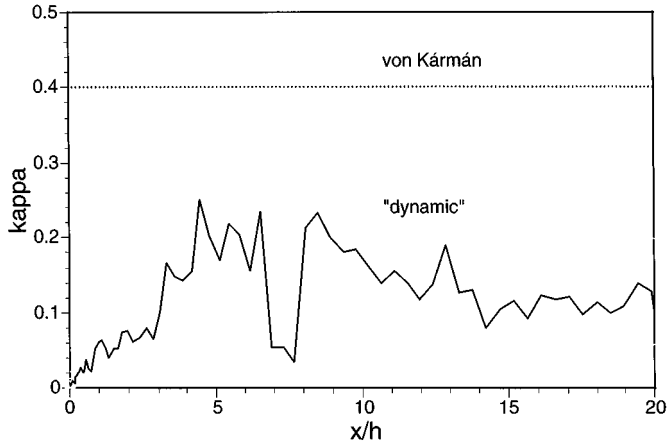

Figure 5. Instantaneous span-averaged dynamic κ in Equation (12) used in the TBLE model *versus* its standard value of the von Kármán constant.

The wall stress on the bottom wall was computed with a range of models similar to those used in the channel flow, from wall stress models using stress balance (equivalent to the log law in attached regions) to the full thin boundary layer equations (2). The horizontal grid for the inner solution was twice as coarse as the outer LES grid in each direction, with averaging and interpolation used to pass information between grids. In addition, simulations using the TBLE wall model were also run in which κ in Equation (5) was modified "dynamically" to account for the fact that the Reynolds stress carried by the nonlinear terms in Equation (2) is significant [12]. This was done by using the outer flow solution ($\overline{\mathbf{u}}$) near the wall to compute the stress predicted by the inner mixing length eddy viscosity model, $\kappa y \widetilde{\overline{u}}_\tau \widetilde{\overline{\mathbf{S}}}$, where $\widetilde{(\,)}$ denotes filtering at the horizontal scale of the inner solution; for simplicity the damping factor D in Equation (5) was set to unity since $y^+ \gg A+$ in most instances. This expression was equated in a least-squares sense to the total resolved and SGS stress at the same horizontal resolution as the inner solution, $-\widetilde{\overline{\mathbf{u}}\,\overline{\mathbf{u}}} - \widetilde{\tau}$, hence

$$\kappa \sim -\left\langle y \widetilde{\overline{u}}_\tau \widetilde{\overline{\mathbf{S}}} : \left(\widetilde{\overline{\mathbf{u}}\,\overline{\mathbf{u}}} + \widetilde{\tau}\right)\right\rangle \Big/ \left\langle y^2 \widetilde{\overline{u}}_\tau^2 \widetilde{\overline{\mathbf{S}}} : \widetilde{\overline{\mathbf{S}}}\right\rangle, \tag{12}$$

where $\langle\,\rangle$ denotes averaging in the spanwise direction. Equation (12) yielded values of κ a factor of two or more lower than the standard value, as shown for one flow realization in Figure 5. Without this correction it is found that the wall stress dips about 10% lower in the main recirculation region.

As seen in Figure 6 for the friction coefficient C_f along the bottom wall, the case using the stress balance model produces a prediction of C_f in the reverse flow that is too low by almost a factor of 2 compared with the wall-resolved calculation, and the recovery past reattachment is also seen to be too slow. When the wall stress is predicted by the thin boundary layer equations, C_f is slightly too high in the

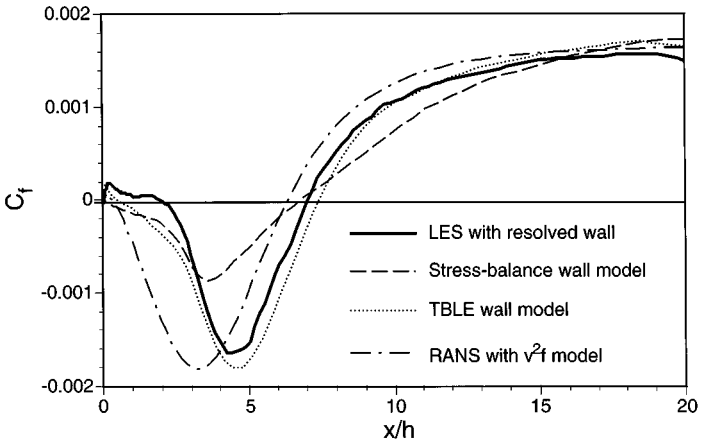

Figure 6. Friction coefficient on the bottom wall behind a step for the wall-resolved LES [2], wall stress models using stress balance and TBLE with a dynamic κ from Equation (12), and a global RANS $v^2 f$ model [18].

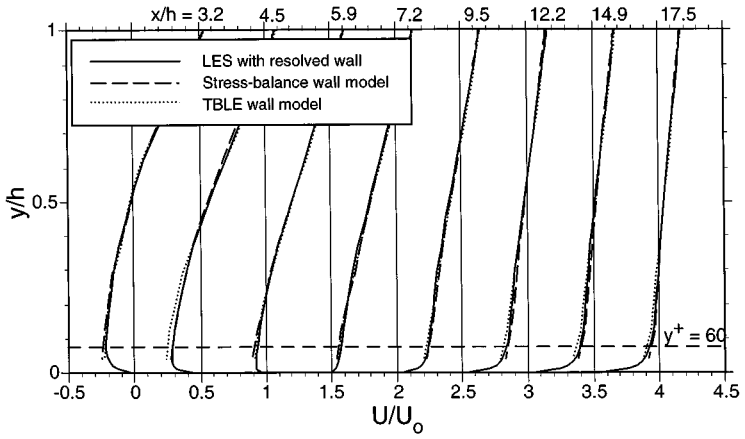

Figure 7. Mean streamwise velocity at different stations behind a step for the wall-resolved LES [2], and stress-balance and TBLE wall stress models. The dashed line is the height of the first computational cell, about 60 wall units near the exit.

reverse flow region, but the shape of the recovery region is predicted better. The effect of C_f being slightly too high in the attached exit region may be related the problem seen in channel flow of too low a slope in the mean streamwise velocity profile near the wall, which for a fixed free stream value causes the near-wall flow to be too rapid and gives too high a value of skin friction. In both wall stress model cases, the reattachment position is in fairly good agreement with the wall-resolved LES results, as are the mean streamwise velocity profiles shown in Figure 7. On the other hand, neither of the cases captured any secondary recirculation in the corner under the step, which may not have been possible anyway on such a coarse

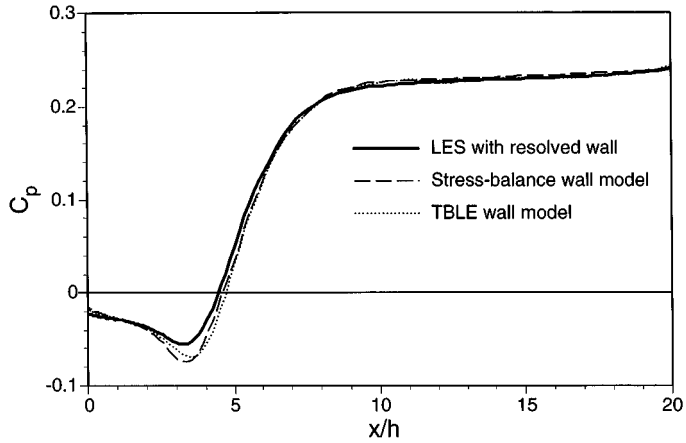

Figure 8. Pressure coefficient on the bottom wall behind a step for the wall-resolved LES [2], and stress-balance and TBLE wall stress models.

grid. The $v^2 f$ RANS model [18], computed for the entire domain, is seen to do a good job in predicting the correct level and shape of the friction coefficient all along the bottom wall, including the separation and recovery regions, as seen in Figure 6; however, the location of the main separation bubble is shifted noticeably. This occurs primarily because the mean core flow is not predicted accurately. The pressure coefficient on the bottom wall behind the step shown in Figure 8 is seen to be slightly lower in the reversed flow region, which reflects the fact that the main recirculation pattern rotates more rapidly in the cases using wall models.

To test the sensitivity of the results in the reverse flow region, exact wall stress data was recorded from the wall-resolved simulation and used as the wall stress model on the coarse gird for a short time. Very little difference in the results was found between doing this and using the TBLE wall model, indicating that the discrepancies in the coarsely resolved flow were due to other factors, such as an inaccurate SGS model near the wall and errors due to the numerical scheme at very coarse resolutions.

The superior skin friction predictions in the reattachment and recovery regions by the thin boundary layer equations compared with the stress balance model are largely the result of having more detailed information about balances between advective terms and large pressure gradients. All the different terms in the momentum equation are comparable at various points around the separated region and the correct balance is required to determine the wall stress accurately. However, the fact that the thin boundary layer equation model is as successful as it is in the primary separated region is somewhat fortuitous, since it describes the inner velocity profile there as a modified log law as a result of the mixing length eddy viscosity imposed, whereas in reality this rapid reverse flow resembles a near-wall jet. In fact, the peak of this “large-scale”, jet-like flow feature in the reverse flow region near the wall was not even resolved in the coarse LES (Figure 7). In order to represent this region

more accurately, the peak of this profile should be properly resolved, and, to obtain better wall stress predictions, more appropriate models should be used, e.g., based on wall jet scaling relations (cf. [30]).

Simple stress balance models, with and without the pressure gradient, have also been applied to trailing edge flow over a hydrofoil, which features a mild separation, with fairly good results [46]. The separation point is well predicted compared with a wall-resolved LES and experimental data, although there are some discrepancies in the mean velocity profiles in the separated region. Adding the pressure gradient term to the stress balance was found to improve the skin friction results in the adverse pressure gradient region; but, as in the case of the flow behind the step, a more accurate allowance for balancing advection terms in this region is needed for further improvements.

In flow simulations of this type, the issue of providing consistent inflow conditions also arises. To avoid large transients in the inlet region, which can adversely affect results downstream and make it difficult to compare with other simulation or experimental data with any consistency, the inflow conditions should be as compatible as possible with the LES simulation, preferably computed with the same resolution, numerical scheme, and SGS and wall models. The problem also remains that the near-wall momentum predicted on coarse LES grids tends to be too high relative to the free stream, which could act to delay separation.

3.3. Model development strategies using optimal control techniques

Because there are many modelling inaccuracies near the coarsely resolved wall in addition to errors from the numerical scheme, it is not surprising that the flow develops a spurious transition zone, even if the exact wall stresses were used. Nicoud et al. [37, 38] posed the question: What wall stresses would actually be required in channel flow to obtain a good mean velocity profile? A suboptimal control strategy [10] was used to determine the wall stresses that would match a predefined log law in channel flow with $\mathrm{Re}_\tau = 4000$ and 20000 on a very coarse grid (32^3 computational cells with a second-order finite difference scheme). The scheme was *suboptimal* in that it enforced the log law at each time step rather than in the mean.

The resulting wall stresses were subjected to a linear regression scheme similar to [7] which correlated them to the velocity field in the near-wall region. This scheme showed that the optimized wall stresses seemed to be correlated with velocity gradients that have no obvious physical interpretation in terms of strain or vorticity. The pattern of wall stresses does not exhibit the streaky structure found in well resolved near-wall regions at physical scales or in poorly resolved near-wall regions at grid scales. The correlations were found to be largely dependent on the grid rather than physical scales, which is not surprising considering the large influence of numerical errors in this region. More surprising was the finding

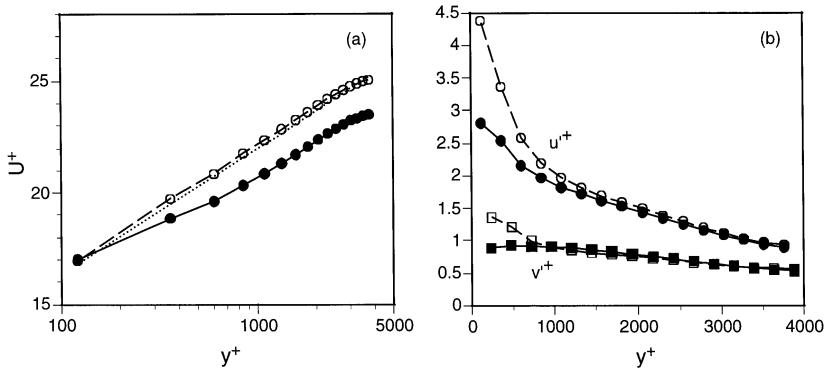

Figure 9. Comparison of channel flow results for an optimized wall stress model [37, 38] (open symbols) and the shifted log law wall stress model [40] (solid symbols) for LES on a 32^3 mesh at $\mathrm{Re}_\tau = 4000$: (a) mean streamwise velocity in wall units, with the log law (Equation (1)) using $\kappa = 0.41$ and $B = 5.1$ for comparison (dotted line); (b) resolved streamwise and wall-normal velocity fluctuation intensities.

that, when the leading correlation terms are used in actual simulations, good mean velocity profiles are predicted for a wide range of Reynolds numbers ($\mathrm{Re}_\tau = 180$–20000) even when the wall stresses were "trained" for one particular Reynolds number. The mean velocity profile using the wall stress models based on the optimized stresses and Piomelli et al.'s [40] shifted log law model are compared in Figure 9a. The optimized wall stresses contain a very high level of fluctuations that also translates into overly high velocity fluctuations near the wall, as seen in Figure 9b for the resolved velocity fluctuation intensities.

It would be interesting to extend this work by optimizing stresses not only at the wall but distributed throughout the near-wall region in an attempt to address the deficiencies in the SGS models, and to determine if there is any useful near-wall model that could be constructed from the results.

4. Conclusions

Results from large-eddy simulations of turbulent wall-bounded flow on very coarse grids with second-order finite-difference schemes using wall stress models have been reviewed. The results in the core of the flows are generally quite good when the mean wall stresses are predicted with sufficient accuracy, despite the low order of the numerical scheme, as seen in simulations of the flow over a step in Section 3.2. Some outer flow features, like the wake profiles in channels, require more resolution to be predicted accurately. In general there must be sufficient resolution to capture scales containing most of the energy, Reynolds shear stresses, and energy transfer. Such resolution requirements are exacerbated in low-order numerical schemes because the high wavenumbers are contaminated by dispersion errors.

There are some perhaps unavoidable discrepancies in the mean flow predictions in the first few off-wall grid points, where current subgrid-scale models are inadequate and numerical errors are large. Despite the success of wall models based on the law of the wall to predict wall stresses in some separated flow cases, improvements are still needed in the modelling of wall stresses in flows experiencing separation, reattachment, and recovery, since standard RANS models based on a law of the wall eddy viscosity are clearly invalid there. A simple "engineering" solution for general flow conditions may be to use several different scaling laws for different flow regimes, which are patched together and activated through some detection mechanism of outer flow conditions. Another solution is to apply much more sophisticated RANS models to determine the wall stresses.

One of the most glaring problems that arises is the inability to predict the near-wall subgrid-scale stresses in the outer flow reliably using standard models, including the dynamic procedure. The reasons for this are: standard SGS models are designed for isotropic flows in which the large, energy-containing scales are resolved adequately, and the physically unrealistic flow that develops on the coarse near-wall mesh cannot be used as a basis for constructing any model quantities, even dynamic coefficients, accurately. Even if accurate model stresses were supplied in the near-wall region, numerical errors from the second-order finite-differencing method degrade the effective resolution to a point where the accuracy of the first few off-wall points is degraded. Solutions for mean flow quantities throughout the near-wall region – not only wall stresses – will need to be computed from trustworthy RANS solutions matched to the core flow beyond this contaminated region. In simple flows like the channel, these quantities can be determined a posteriori. For flows with developing boundary layers or separated flow, or in other cases where the flow depends more critically on the near-wall behaviour, an iterative strategy may be required in which a RANS model, matched to long-time averages of the outer flow, is computed occasionally to correct the mean wall stresses.

Wall modelling studies are still needed using simulations with high fidelity numerical methods (e.g., spectral-spline [27]) to separate issues of numerical resolution and errors from actual wall model performance. There is also ample high Reynolds number data from turbulent pipe flow experiments for both smooth and rough walls [1, 39, 49], and it would be useful to test the performance of coarse LES in these flows using low-order finite-difference as well as higher fidelity numerical methods. We may also be able to gain some insight from the experimental data into the general effects of wall models by observing the effects of wall roughness. Ultimately, we want to incorporate wall roughness effects in an accurate way into the wall models.

The overarching question of whether wall models in LES can be considered to be successful or not at this time is rather subjective, since what is deemed acceptable depends on the flow problem at hand, the quantities one is interested in,

and one's tolerance for error. But, with regard to numerical resolution, it appears in many cases that the old adage, "you get what you pay for", still applies.

Acknowledgements

The authors gratefully acknowledge the many stimulating discussions and valuable contributions of their colleagues Professors J. Jiménez and J.S. Baggett in this course of this research over the last several years. This work has been supported by AFOSR Grant F49620-97-1-0210.

References

1. AGARD, A selection of test cases for the validation of large-eddy simulations of turbulent flows. Advisory Report 345, NATO (1998), Chap. 5, pp. 109–128.
2. Akselvoll, K. and Moin, P., Large eddy simulation of turbulent confined coannular jets and turbulent flow over a backward facing step. Technical Report TF-63, Department of Mechanical Engineering, Stanford, CA (1995).
3. Arnal, M. and Friedrich, R., Large-eddy simulation of a turbulent flow with separation. In: Durst, F., Friedrich, R., Launder, B.E., Schmidt, F.W., Schumann, U. and Whitelaw, J.H. (eds), *Selected Papers from the Eighth Symposium on Turbulent Shear Flows*. Springer-Verlag, New York (1993) pp. 169–187.
4. Baggett, J.S., Jiménez, J. and Kravchenko, A.G., Resolution requirements in large-eddy simulations of shear flows. In: *Annual Research Briefs*. Center for Turbulence Research, Stanford, CA (1997) pp. 51–66.
5. Baggett, J.S., Some modeling requirements for wall models in large eddy simulation. In: *Annual Research Briefs*. Center for Turbulence Research, Stanford, CA (1997) pp. 123–134.
6. Baggett, J.S., On the feasibility of merging LES with RANS for the near-wall region of attached turbulent flows. In: *Annual Research Briefs*. Center for Turbulence Research, Stanford, CA (1998) pp. 267–277.
7. Bagwell, T.G., Adrian, R.J., Moser, R.D. and Kim, J., Improved approximation of wall shear stress boundary conditions for large eddy simulation. In: So, R.M.C., Speziale, C.B. and Launder, B.E. (eds), *Near-Wall Turbulent Flows*. Elsevier Science, New York (1993) pp. 265–276.
8. Balaras, E. and Benocci, C., Subgrid scale models in finite difference simulations of complex wall flows. In: *AGARD CP-551* (1994) pp. 2.1–2.6.
9. Balaras, E., Benocci, C. and Piomelli, U., Two-layer approximate boundary conditions for large-eddy simulations. *AIAA J.* **34** (1996) 1111–1119.
10. Bewley, T.R. and Moin, P., Optimal and robust approaches for linear and nonlinear regulation problems in fluid mechanics. AIAA Paper 97-1872 (1997).
11. Cabot, W., Large-eddy simulations with wall models. In: *Annual Research Briefs*. Center for Turbulence Research, Stanford, CA (1995) pp. 41–50.
12. Cabot, W., Near-wall models in large eddy simulations of flow behind a backward-facing step. In: *Annual Research Briefs*. Center for Turbulence Research, Stanford, CA (1996) pp. 199–210.
13. Cabot, W., Wall models in large eddy simulation of separated flow. In: *Annual Research Briefs*. Center for Turbulence Research, Stanford, CA (1997) pp. 97–106.
14. Cabot, W., Jiménez, J. and Baggett, J.S., On wakes and near-wall behavior in coarse large-eddy simulation of channel flow with wall models and second-order finite-difference methods. In: *Annual Research Briefs*. Center for Turbulence Research, Stanford, CA (1999) pp. 343–354.

15. Choi, H. and Moin, P., Effects of the computational time step on numerical simulation of turbulent flow. *J. Comput. Phys.* **113** (1994) 1–4.
16. Dean, R.B., A single formula for the complete velocity profile in a turbulent boundary layer. *ASME J. Fluids Engrg.* **98** (1976) 723–727.
17. Deardorff, J.W., A numerical study of three-dimensional turbulent channel flow at large Reynolds numbers. *J. Fluid Mech.* **41** (1970) 453–480.
18. Durbin, P.A., Near-wall turbulence closure without "damping functions". *Theoret. Comput. Fluid Dynam.* **3** (1991) 1–13.
19. Germano, M., Piomelli, U., Moin, P. and Cabot, W.H., A dynamic subgrid-scale eddy viscosity model. *Phys. Fluids* **3** (1991) 1760–1765. Erratum: *Phys. Fluids* **3** (1991), 3128.
20. Ghosal, S., An analysis of numerical errors in large-eddy simulations of turbulence. *J. Comput. Phys.* **125** (1996) 187–206.
21. Ghosal, S. and Moin, P., The basic equations for the large eddy simulation of turbulent flows in complex geometry. *J. Comput. Phys.* **118** (1995) 24–37.
22. Grötzbach, G., Direct numerical and large eddy simulation of turbulent channel flows. In: Cheremisinoff, N.P. (ed.), *Encyclopedia of Fluid Mechanics* Gulf Publishers, Houston (1987) Chap. 34, pp. 1337–1391.
23. Harlow, F.H. and Welch, J.E., Numerical calculation of time-dependent viscous incompressible flow of fluid with free surface. *Phys. Fluids* **8** (1965) 2182–2189.
24. Hoffmann, G. and Benocci, C., Approximate wall boundary conditions for large eddy simulations. In: Benzi, R. (ed.), *Advances in Turbulence V*, Kluwer Academic Publishers, Dordrecht (1995), pp. 222–228.
25. Kim, J. and Moin, P., Application of a fractional-step method to incompressible Navier–Stokes equations. *J. Comput. Phys.* **177** (1987) 133–166.
26. Kravchenko, A.G. and Moin, P., On the effects of numerical errors in large-eddy simulations of turbulent flows. *J. Comput. Phys.* **59** (1985) 308-323.
27. Kravchenko, A.G., Moin, P. and Moser, R., Zonal embedded grids for numerical simulations of wall-bounded turbulent flows. *J. Comput. Phys.* **127** (1996) 412–423.
28. Jiménez, J. and Moser, R.D., LES: Where we are and what we can expect. AIAA Paper 98-2891 (1998).
29. Jiménez, J. and Vasco, C., Approximate lateral boundary conditions for turbulent simulations. In: Moin, P. and Reynolds, W.C. (eds), *Studying Turbulence Using Numerical Simulation VII*. Center for Turbulence Research, Stanford, CA (1998) pp. 399–412.
30. Le, H., Moin, P. and Kim, J., Direct numerical simulation of turbulent flow over a backward-facing step. *J. Fluid Mech.* **330** (1997) 349–374.
31. Lilly, D., A proposed modification of the Germano subgrid-scale closure method. *Phys. Fluids A* **4** (1992) 633–635.
32. Lund, T.S. and Kaltenbach, H.-J., Experiments with explicit filtering for LES using a finite-difference method. In: *Annual Research Briefs*. Center for Turbulence Research, Stanford, CA (1995) pp. 91–105.
33. Mason, P.J. and Callen, N.S., On the magnitude of the subgrid-scale eddy coefficient in large-eddy simulations of turbulent channel flow. *J. Fluid Mech.* **162** (1986) 439–462.
34. Mason, P.J. and Thomson, D.J., Stochastic backscatter in large-eddy simulations of boundary layers. *J. Fluid Mech.* **242** (1992) 51–78.
35. Nakayama, A., Maeda, K. and Noda, H., Instantaneous and filtered velocity profiles in smooth and rough boundary layers. Preprint (1999).
36. Nicoud, F., Winckelmans, G., Carati, D., Baggett, J. and Cabot, W., Boundary conditions for LES away from the wall. In: Moin, P. and Reynolds, W.C. (eds), *Studying Turbulence Using Numerical Simulation VII*. Center for Turbulence Research, Stanford, CA (1998) pp. 413-422.

37. Nicoud, F. and Baggett, J., On the use of the optimal control theory for deriving wall models for LES. In: *Annual Research Briefs*. Center for Turbulence Research, Stanford, CA (1999) pp. 329–341.
38. Nicoud, F., Baggett, J., Moin, P. and Cabot, W., LES wall-modeling based on optimal control theory. *Phys. Fluids* (2000) submitted.
39. Perry, A.E., Henbest, S.M. and Chong, M.S., A theoretical and experimental study of wall turbulence. *J. Fluid Mech.* **165** (1986) 163–199.
40. Piomelli, U., Ferziger, J., Moin, P. and Kim, J., New approximate boundary conditions for large eddy simulations of wall-bounded flows. *Phys. Fluids* **1** (1989) 1061–1068.
41. Porté-Agel, F., Meneveau, C. and Parlange, M.B., A scale-dependent dynamic model for large-eddy simulation: Application to a neutral atmospheric boundary. *J. Fluid Mech.* (2000) submitted.
42. Schumann, U., Subgrid scale model for finite difference simulations of turbulent flows in plane channels and annuli. *J. Comput. Phys.* **18** (1975) 376–404.
43. Smagorinsky, J., General circulation experiments with the primitive equations. I. The basic experiment. *Mon. Weather Rev.* **91** (1963) 499–164.
44. Sullivan, P.P., McWilliams, J.C. and Moeng, C.-H., A grid nesting method for large-eddy simulation of planetary boundary-layer flows. *Boundary-Layer Met.* **80** (1996) 167–202.
45. Vasilyev, O.V., Lund, T.S. and Moin, P., A general class of commutative filters for LES in complex geometries. *J. Comput. Phys.* **146** (1998) 82–104.
46. Wang, M., LES with wall model for trailing-edge aeroacoustics. In: *Annual Research Briefs*. Center for Turbulence Research, Stanford, CA (1999) pp. 355–364.
47. Werner, H. and Wengle, H., Large-eddy simulation of turbulent flow over and around a cube in a plate channel. In: Durst, F., Friedrich, R., Launder, B.E., Schmidt, F.W., Schumann, U. and Whitelaw, J.H. (eds), *Selected Papers from the Eighth Symposium on Turbulent Shear Flows*. Springer-Verlag, New York (1993) pp. 155–168.
48. Wu, X. and Squires, K.D., Prediction of the three-dimensional turbulent boundary layer over a swept bump. *AIAA J.* **36** (1998) 505–514.
49. Zagarola, M.V. and Smits, A.J., Scaling of the mean velocity profile for turbulent pipe flow. *Phys. Rev. Lett.* **78** (1997) 239–242.
50. Zang, Y., Street, R.L. and Koseff, J.R., A dynamic mixed subgrid-scale model and its application to turbulent recirculating flows. *Phys. Fluids A* **5** (1993) 3186–3196.